

Electronic Supplementary Information for:

Carborane-based heteromolecular extended networks driven by directional Te•••N chalcogen-bonding interactions

Maxime Beau,^a Olivier Jeannin,^a Marc Fourmigué,^{*a} Emmanuel Aubert,^b Enrique Espinosa,^b Sunhee Lee,^c Won-Sik Han,^c Je-Rang Jeon^{*a}

^aUniv Rennes, CNRS, ISCR (Institut des Sciences Chimiques de Rennes), Campus de Beaulieu, 35000 Rennes, France.

^bUniversité de Lorraine, CNRS, CRM2, F-54000 Nancy, France.

^cDepartment of Chemistry, Seoul Women's University, Seoul 01797, Republic of Korea.

marc.fourmigue@univ-rennes.fr

je-rang.jeon@univ-rennes.fr

Table of Contents

Experimental Section	S2
Table S1: Crystallographic table	S4
Figure S1: <i>Nido</i> -cage-based noncovalent interactions in $[nido-7,8-(SeMe)_2C_2B_9H_{10}]^-(Hbipy-pip)^+$	S5
Figure S2: <i>Nido</i> -cage-based noncovalent interactions in $[nido-7,8-I_2C_2B_9H_{10}]^-(Hbpe)^+$	S5
Figure S3: Structures of $[nido-7,8-I_2C_2B_9H_{10}]^-(Hbpe)^+$ and $[nido-7,8-(SeMe)_2C_2B_9H_{10}]^-(Hbipy-pip)^+$	S6
Figure S4: Structure of 3•bpe	S7
Figure S5: Optimized structures of 3•bpe and 4•bpe	S8
Figure S6: ESP map of 4	S8
References	S9

Experimental Section

1. General considerations and cocrystallization

Reagents were obtained from commercial suppliers and used without further purification. Solvents were dried using commercial solvent purification system from Inert Technology. **1–3** were prepared as described in the literature.¹ The solution cocrystallizations for [*nido*-7,8- $I_2C_2B_9H_{10}$](Hbpe⁺), [*nido*-7,8-(SeMe) $_2C_2B_9H_{10}$](Hbipy-pip⁺), and **3**•bipy-pip, were performed in a glass vial of 12 mm diameter. Single crystals of **3**•bpe and **4**•bpe were obtained through the co-sublimation method.² Crystals were systematically obtained together with starting compounds, hindering the isolation of a bulk sample for elemental analysis.

[*nido*-7,8- $I_2C_2B_9H_{10}$](Hbpe⁺). 1 (7 mg, 0.018 mmol) and 1,2-bis(4-pyridyl)ethane (bpe, 3.5 mg, 0.019 mmol) were solubilized in a 1:1 mixed solvent (7 mL) of EtOAc and iPrOH. The glass tube was left open for slow evaporation on a period of 7 days. Colorless prism-shaped crystals of [*nido*-7,8- $I_2C_2B_9H_{10}$](Hbpe⁺) suitable for single-crystal X-ray diffraction were collected from the bottom of the vial.

[*nido*-7,8-(SeMe) $_2C_2B_9H_{10}$](Hbipy-pip⁺). 2 (5 mg, 0.016 mmol) and 1,4-di(4-pyridyl)piperazine (bipy-pip, 5 mg, 0.021 mmol) were solubilized in a 1:1 mixed solvent (4 mL) of EtOH and Et₂O. The glass tube was left open for slow evaporation on a period of 7 days. Colorless plate-shaped crystals of *nido*-7,8-(SeMe) $_2C_2B_9H_{10}$](Hbipy-pip⁺) suitable for single-crystal X-ray diffraction were collected from the bottom of the vial.

3•bipy-pip. 3 (10 mg, 0.024 mmol) and 1,4-di(4-pyridyl)piperazine (bipy-pip, 5 mg, 0.021 mmol) were solubilized in EtOH (3 mL) with 3 drops of CH₂Cl₂. The glass tube was left open for slow evaporation on a period of 3 days. Colorless plate-shaped crystals of *nido*-7,8-(SeMe) $_2C_2B_9H_{10}$](Hbipy-pip⁺) suitable for single-crystal X-ray diffraction were collected from the bottom of the vial.

3•bpe and 4•bpe. 3 (15 mg, 0.036 mmol) and 1,2-bis(4-pyridyl)ethane (bpe, 15 mg, 0.081 mmol) were placed at each end of a vacuum-sealed glass tube (10⁻⁵ mbar). The temperature for each end was gradually increased from 40 to 85 °C over two weeks. **3**•bpe was obtained as pale-yellow prism-shaped crystals in the middle of the tube with a minor presence of **4**•bpe as colorless prism-shaped crystals.

2. Single crystal X-ray diffraction analysis

Single crystals that are suitable for X-ray analysis were coated with Paratone-N oil and mounted on a MicroMounts™ rod. X-ray diffraction measurements were performed on a Bruker APEX II diffractometer for [*nido*-7,8- $I_2C_2B_9H_{10}$](Hbpe⁺), [*nido*-7,8-(SeMe) $_2C_2B_9H_{10}$](Hbipy-pip⁺), **3**•bipy-pip, and **3**•bpe and on a Bruker D8 Venture diffractometer for **4**•bpe, both operating with a Mo K α ($\lambda = 0.71073$ Å) X-ray tube with a graphite monochromator. The structures were solved (SHELXT-2014) by dual space methods and refined (SHELXL-2014/7) by full-matrix least-squares procedures on F².³ All non-H atoms of the donor molecules were refined anisotropically. The –NH Hydrogen atoms of [*nido*-7,8- $I_2C_2B_9H_{10}$](Hbpe⁺) and [*nido*-7,8-(SeMe) $_2C_2B_9H_{10}$](Hbipy-pip⁺) were refined, and all other hydrogen atoms were introduced at calculated positions (riding model), included in structure factor calculations but not refined. Thermal parameters were refined anisotropically for all non-hydrogen atoms. Crystallographic data and the details of data collection are listed in Table S1.

3. Theoretical Calculations

Theoretical calculations were performed on isolated molecules using the Gaussian16 software⁴ at the Density level of Theory employing the B3LYP functional and the Def2TZVPP basis set (pseudo potentials were used for the heavier Te & I atoms). Empirical dispersion was taken into account with the Grimme's original D3 damping function.⁵ Frequency calculations were performed to check that true energy minima were obtained. Electrostatic potential (ESP) mapped on the 0.001a.u. isodensity surface were then computed with the AIMAll software package;⁶ the maximum of ESP $V_{S,max}$ in the region of the σ -holes associated with I, Se and Te atoms were located using MWFN software.⁷

Crystal structures of 3•(bpe) and 4•(bpe) were optimized through periodic DFT calculations using CASTEP 19.11 software.⁸ The PBE exchange and correlation functional was used, complemented by semi-empirical dispersion corrections.⁹ Ultrasoft pseudopotentials generated "on-the-fly" were used. A *precise* plane wave cut off was used, corresponding to a limit of 588 eV. The MP grid size was set to 5 3 2. The optimization convergence criteria were fixed as follows: maximal stress tolerance at convergence $5 \cdot 10^{-3}$ GPa, energy shift $5 \cdot 10^{-6}$ eV, force $25 \cdot 10^{-3}$ a.u., displacement $5 \cdot 10^{-4}$ Å.

Table S1 | Crystallographic data

	[<i>nido</i> -7,8- I ₂ C ₂ B ₉ H ₁₀](Hbpe)	[<i>nido</i> -7,8- (SeMe) ₂ C ₂ B ₉ H ₁₀](Hbi py-pip)	3•bipy-pip	3•bpe	4•bpe
Empirical formula	C ₁₇ H ₃₁ B ₉ I ₂ N ₂ O	C ₁₈ H ₃₃ B ₉ N ₄ Se ₂	C ₁₈ H ₃₂ B ₁₀ N ₄ Te ₂	C ₁₆ H ₂₈ B ₁₀ N ₂ Te ₂	C ₁₅ H ₂₅ B ₁₀ N ₂ Te
Formula weight, g mol ⁻¹	630.53	560.69	667.77	611.7	469.07
Crystal system	Monoclinic	Triclinic	Monoclinic	Monoclinic	Triclinic
Space group	P2 ₁ /n	P-1	P2 ₁ /m	P2 ₁ /n	P-1
Wavelength, Å	0.71073	0.71073	0.71073	0.71073	0.71073
Temperature, K	150	296	296	296	150
<i>a</i> , Å	11.8500(7)	9.4316(4)	8.154(1)	8.3930(9)	6.8598(4)
<i>b</i> , Å	12.0645(8)	11.7393(6)	22.026(3)	19.778(3)	9.2021(5)
<i>c</i> , Å	18.803(1)	13.1695(7)	8.351(1)	15.502(2)	17.658(1)
α , °	90	91.699(2)	90	90	91.921(2)
β , °	105.424(3)	107.070(1)	114.634(4)	98.526(5)	91.798(2)
γ , °	90	110.878(1)	90	90	95.622(2)
<i>V</i> , Å ³	2591.4(3)	1287.6(1)	1363.4(3)	2544.8(5)	1108.0(1)
<i>Z</i>	4	2	2	4	2
ρ_{calcd} , Mg m ⁻³	1.616	1.446	1.627	1.597	1.406
μ , mm ⁻¹	2.440	2.887	2.155	2.299	1.345
Reflections coll./unique	19752/3581	31649/4668	9902/1531	20226/4230	9018/4710
<i>R</i> (int)	0.0602	0.0284	0.1078	0.0539	0.1088
^a <i>R</i> ₁ (<i>I</i> > 2σ(<i>I</i>))	0.0469	0.0353	0.0594	0.0623	0.0258
^b w <i>R</i> ₂ (all)	0.1067	0.0934	0.1172	0.2116	0.0645
GoF	1.032	1.072	0.978	1.065	1.102

$$^a R_1 = \sum ||F_0| - |F_c|| / \sum |F_0|, \text{ and } ^b wR_2 = [\sum w(F_0^2 - F_c^2)^2 / \sum w(F_0^2)^2]^{1/2}$$

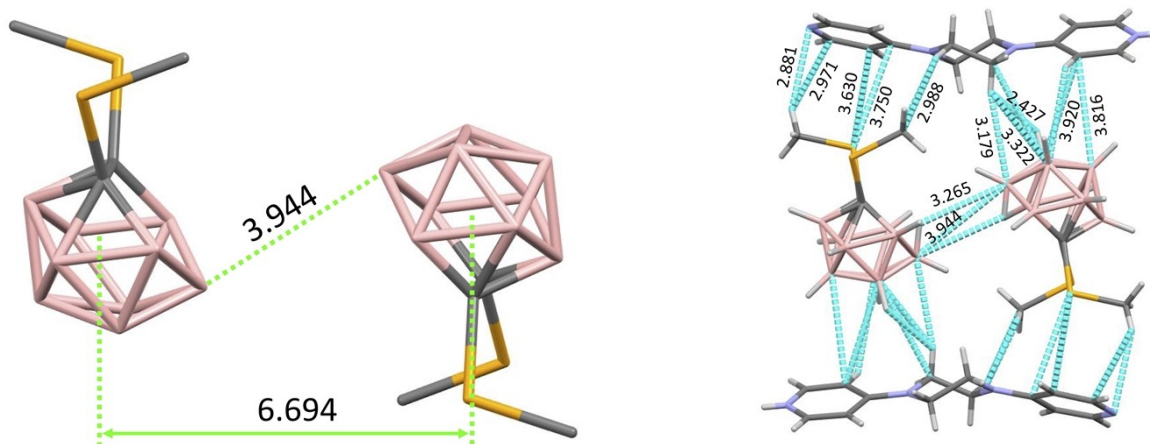


Figure S1 | Crystal packing structures of $[nido-7,8-(SeMe)_2C_2B_9H_{10}]^-(Hbipy-pip)^+$ (blue, nitrogen; dark gray, carbon; pink, boron; light gray, hydrogen). The contacting distances of the noncovalent bonds are indicated with light green and cyan dashed lines with the distances in Å. The cage⁻•••cage⁻ interaction¹⁰ distance is found to be 6.694 Å.

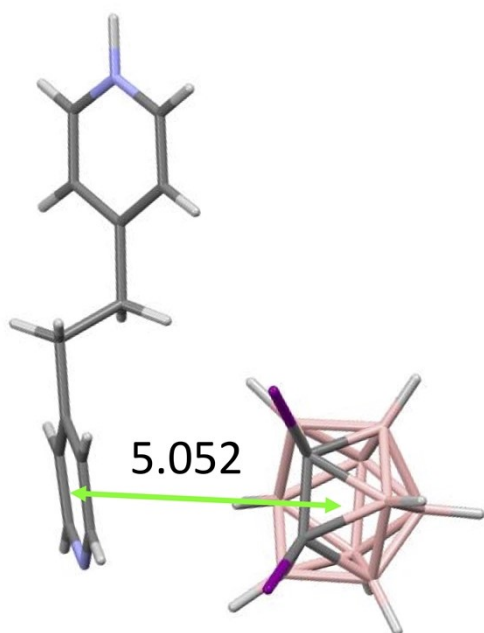


Figure S2 | Crystal packing structure of $[nido-7,8-I_2C_2B_9H_{10}]^-(Hbpe)^+$ (blue, nitrogen; dark gray, carbon; pink, boron; light gray, hydrogen). The contacting distances of the noncovalent bonds are indicated with light green and cyan dashed lines with the distances in Å. The cage⁻••• π interaction¹¹ distance is found to be 5.052 Å.

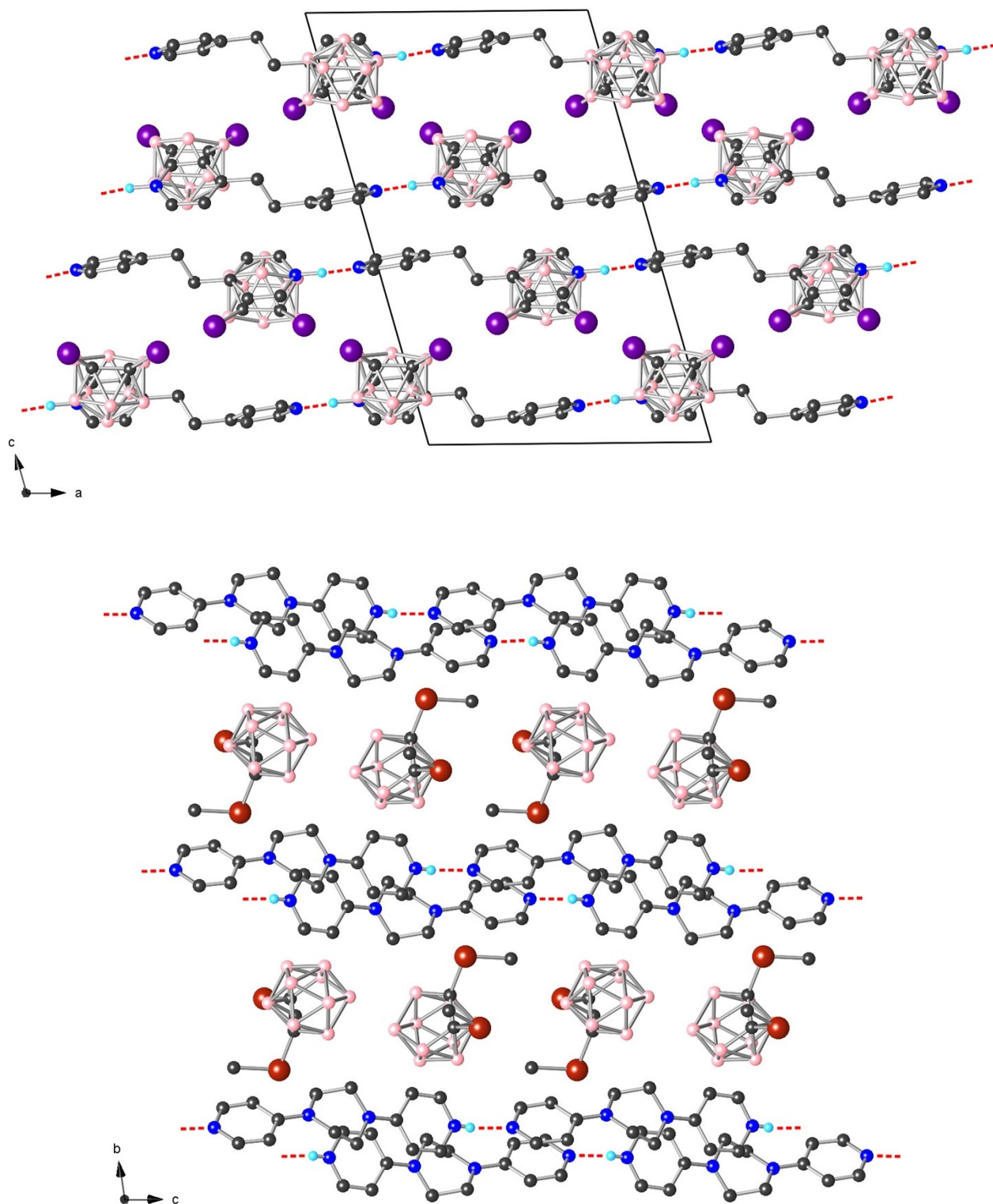


Figure S3 | Structures of $[nido-7,8-I_2C_2B_9H_{10}]^-(Hbpe)^+$ (upper) and $[nido-7,8-(SeMe)_2C_2B_9H_{10}]^-(Hbipy-pip)^+$ (lower) with HB interactions in red dotted lines. Purple, brick, blue, black, pink, and cyan spheres represent I, Se, N, C, B, and H atoms, respectively. H atoms, except for those on $-NH$, are omitted for clarity.

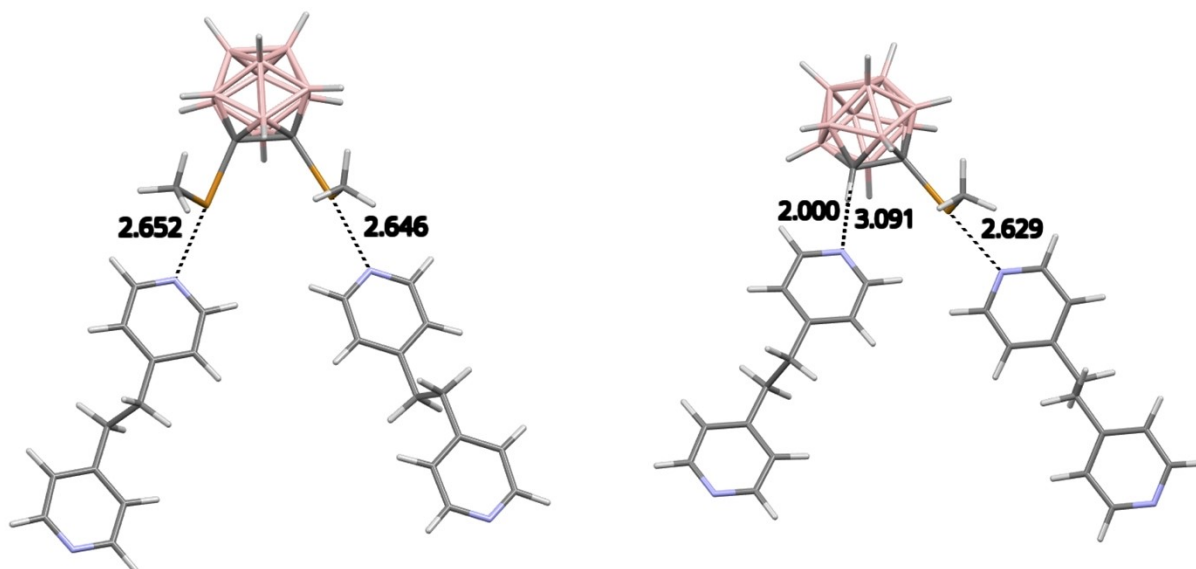


Figure S5 | Optimized structures of **3•(bpe)** (left) and **4•(bpe)** (right) obtained through the periodic DFT calculations

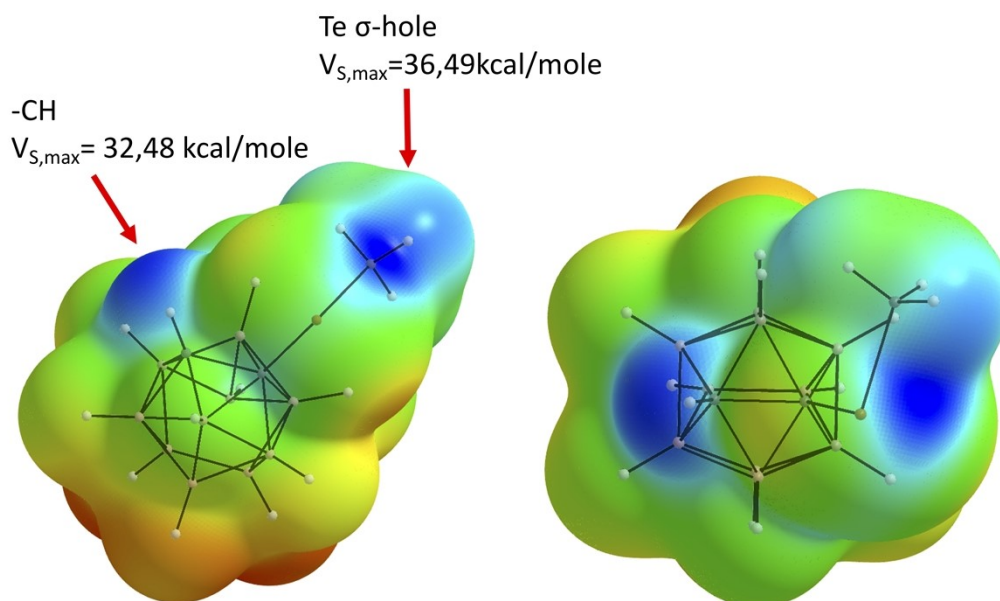


Figure S6 | ESP mapped on the 0.001 a.u. isodensity surface of **4** with the ESP range of -15.7 (red) and $+34.5$ kcal/mol (blue). Note that these values can be compared with the one of a prototypical organic halogen bond donor, iodopentafluorobenzene (33.0 kcal/mol), in the same calculation conditions.¹

-
- (1) M. Beau, S. Lee, S. Kim, W.-S. Han, O. Jeannin, M. Fourmigué, E. Aubert, E. Espinosa, I.-R. Jeon, *Angew. Chem. Int. Ed.*, 2021, **60**, 366.
 - (2) For details, see: P. M. J. Szell, S. A. Gabriel, E. Caron-Poulin, O. Jeannin, M. Fourmigué and D. L. Bryce, *Cryst. Growth Des.* 2018, **18**, 6227.
 - (3) Sheldrick, G. M. Programs for the Refinement of Crystal Structures; University of Göttingen: Göttingen, Germany, 1996.
 - (4) Gaussian 16, Revision C.01, M. J. Frisch, G. W. Trucks, H. B. Schlegel, G. E. Scuseria, M. A. Robb, J. R. Cheeseman, G. Scalmani, V. Barone, G. A. Petersson, H. Nakatsuji, X. Li, M. Caricato, A. V. Marenich, J. Bloino, B. G. Janesko, R. Gomperts, B. Mennucci, H. P. Hratchian, J. V. Ortiz, A. F. Izmaylov, J. L. Sonnenberg, D. Williams-Young, F. Ding, F. Lipparini, F. Egidi, J. Goings, B. Peng, A. Petrone, T. Henderson, D. Ranasinghe, V. G. Zakrzewski, J. Gao, N. Rega, G. Zheng, W. Liang, M. Hada, M. Ehara, K. Toyota, R. Fukuda, J. Hasegawa, M. Ishida, T. Nakajima, Y. Honda, O. Kitao, H. Nakai, T. Vreven, K. Throssell, J. A. Montgomery, Jr., J. E. Peralta, F. Ogliaro, M. J. Bearpark, J. J. Heyd, E. N. Brothers, K. N. Kudin, V. N. Staroverov, T. A. Keith, R. Kobayashi, J. Normand, K. Raghavachari, A. P. Rendell, J. C. Burant, S. S. Iyengar, J. Tomasi, M. Cossi, J. M. Millam, M. Klene, C. Adamo, R. Cammi, J. W. Ochterski, R. L. Martin, K. Morokuma, O. Farkas, J. B. Foresman, and D. J. Fox, Gaussian, Inc., Wallingford CT, 2019.
 - (5) S. Grimme, J. Antony, S. Ehrlich and H. Krieg, *J. Chem. Phys.* 2010, **132**, 154104.
 - (6) AIMAll (Version 19.10.12), Todd A. Keith, TK Gristmill Software, Overland Park KS, USA, 2019 (aim.tkgristmill.com)
 - (7) T. Lu, F. Chen, *J. Mol. Graph. Model.* 2012, **38**, 314.
 - (8) S. J. Clark, M. D. Segall, C. J. Pickard, P. J. Hasnip, M. J. Probert, K. Refson, M. C. Payne "First principles methods using CASTEP" *Zeitschrift fuer Kristallographie*, 2005, 220(5-6), 567-570.
 - (9) Grimme, S. *J. Comput. Chem.* 2006, **27**, 1787.
 - (10) D. Tu, J. Li, F. Sun, H. Yan, J. Poater, M. Solà, *JACS Au*, 2021, **1**, 2047.
 - (11) D. Tu, H. Yan, J. Poater, M. Solà, *Angew. Chem. Int. Ed.*, 2020, **59**, 9018.